Electronic Supplementary Material (ESI) for Journal of Materials Chemistry A.

Electronic Supplementary Information

High-performance $LiTi_2(PO_4)_3$ anode for high-areal-capacity flexible aqueous lithium-ion batteries

Guo-Ming Weng, Long-Yin Simon Tam and Yi-Chun Lu*

Electrochemical Energy and Interfaces Laboratory, Department of Mechanical and Automation Engineering, The Chinese University of Hong Kong, Shatin, N. T. 999077, Hong Kong SAR, China

*E-mail: yichunlu@mae.cuhk.edu.hk

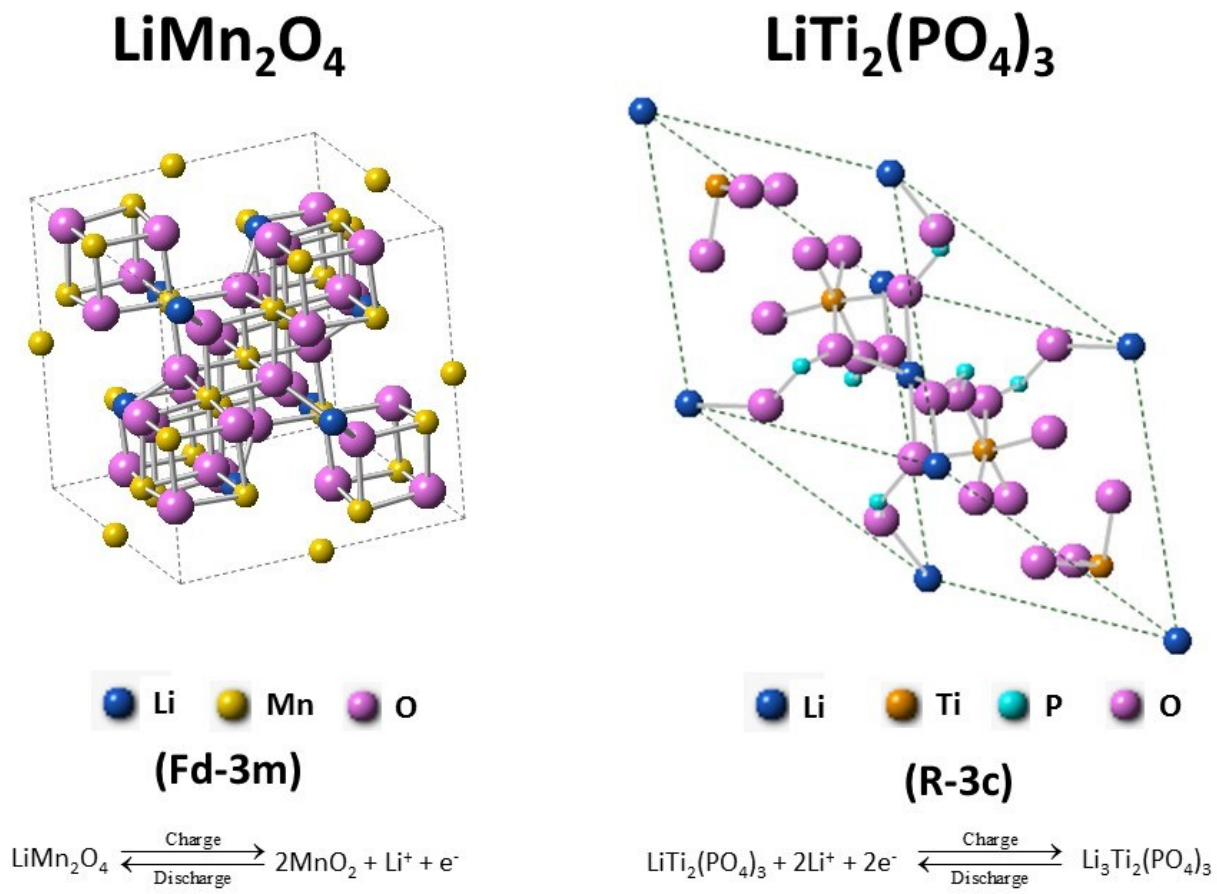

Figure S1. Crystal structure and reaction scheme of $LiMn_2O_4$ and $LiTi_2(PO_4)_3$.

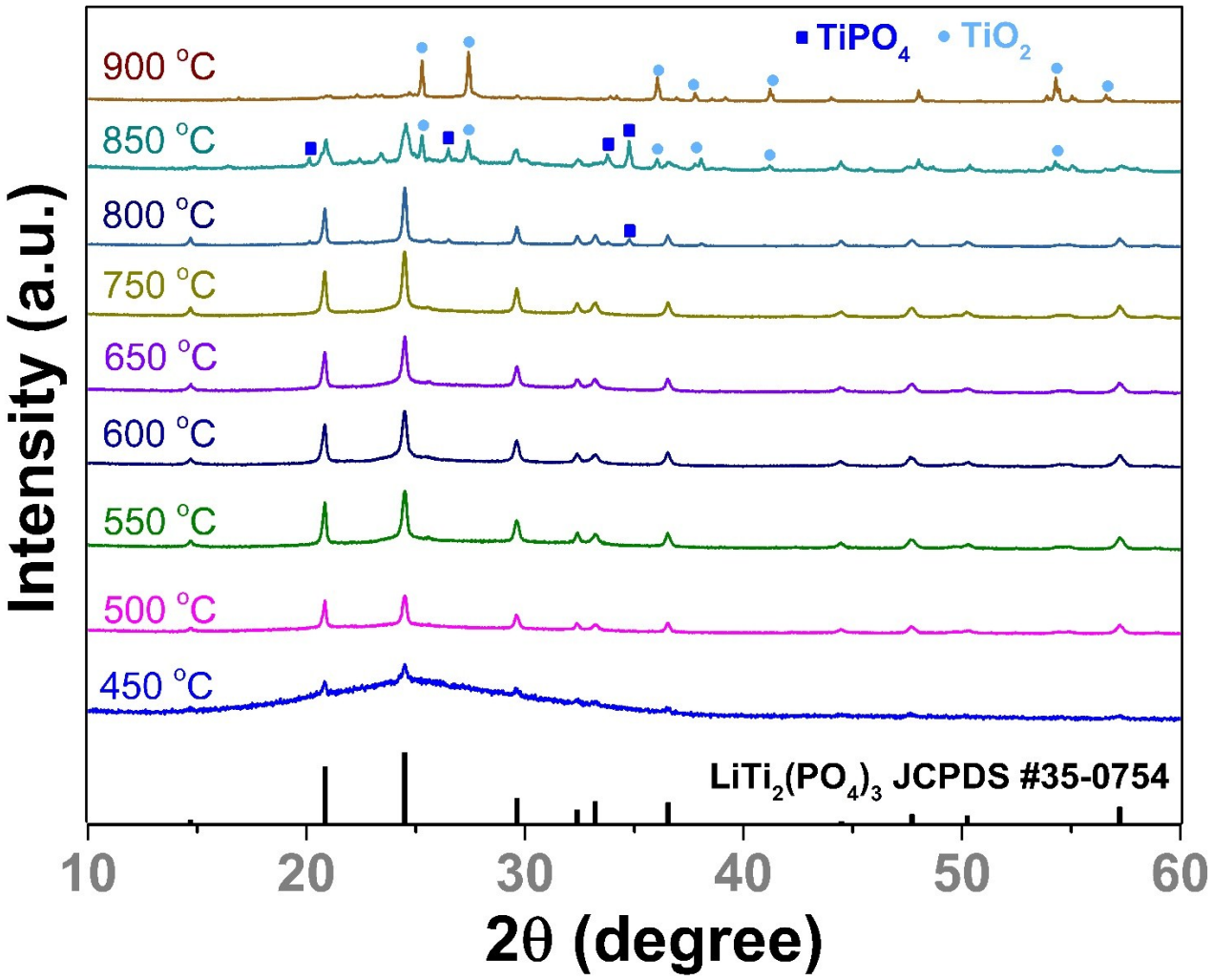

Figure S2. XRD spectra of ccLTPs obtained at specified calcination temperatures.

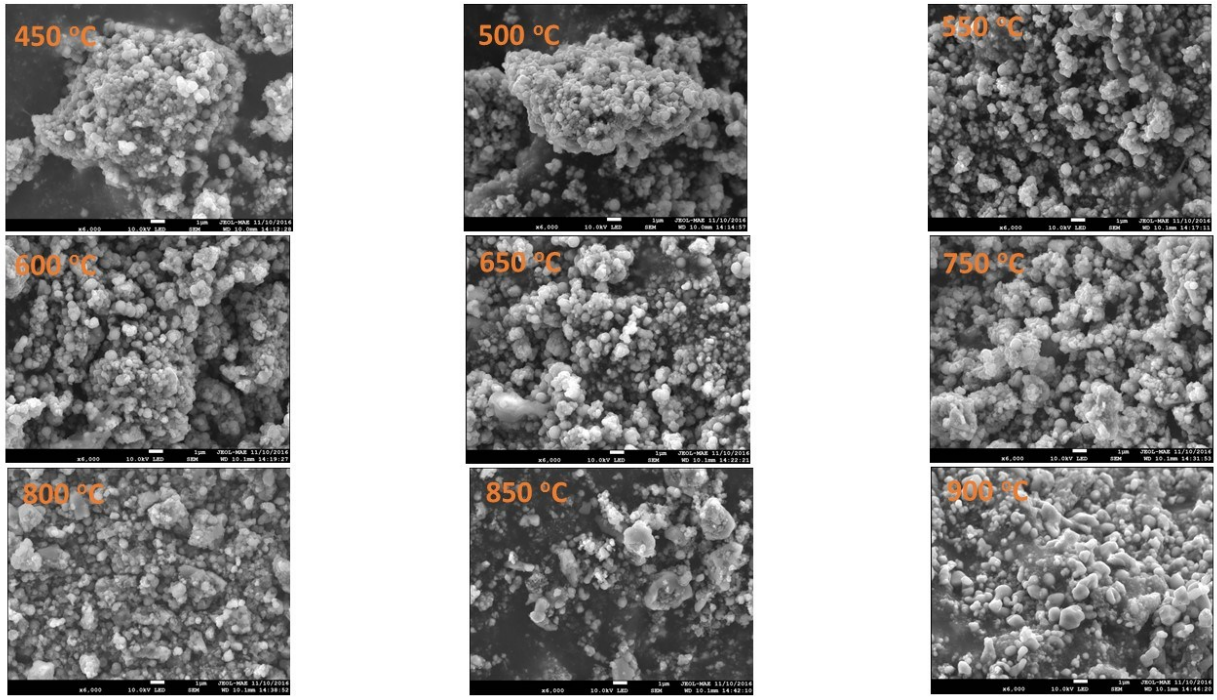

Figure S3. SEM images of ccLTPs obtained at specified calcination temperatures. The scale bars are the same at 1 μm. The agglomeration observed in the samples of 450 °C and 500 °C could be caused by the remaining sticky macromolecular aromatic ring compounds [1] owing to incomplete decomposition of the pitch. The thermal decomposition of pitch can be completed at temperatures higher than 550 °C (Fig. S4), in which case the agglomeration was greatly alleviated.

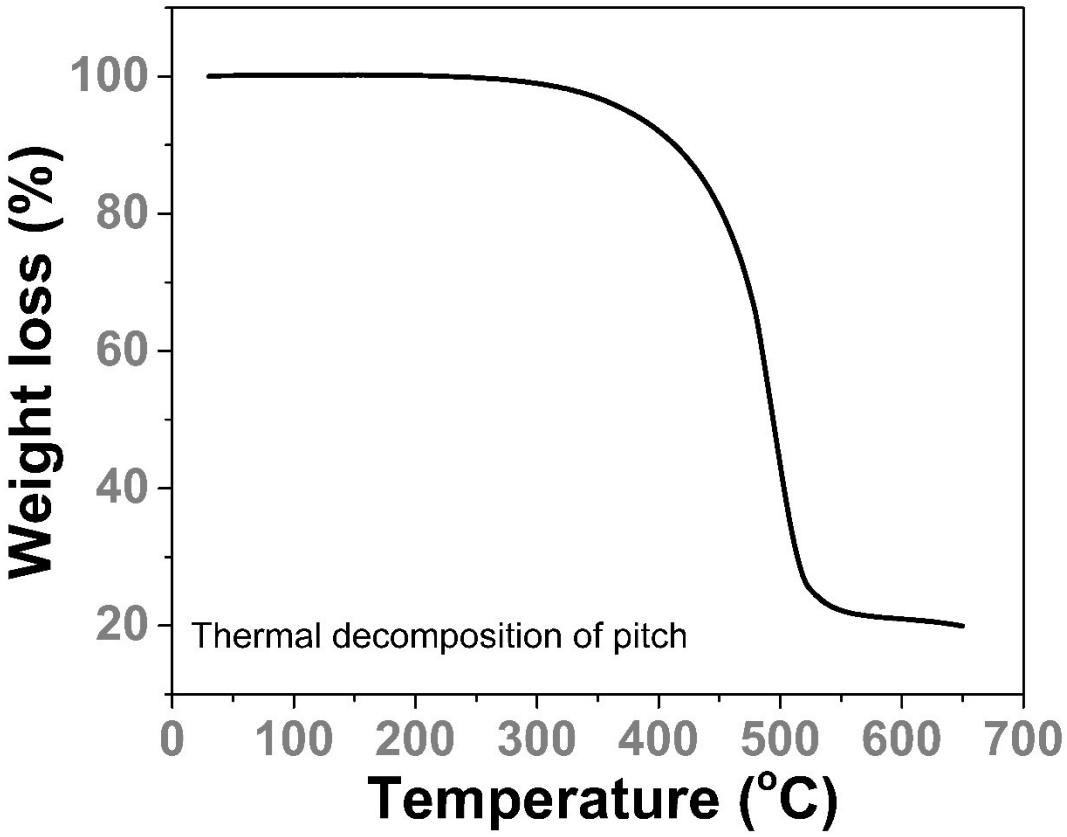

Figure S4. TGA spectrum of the pitch in pure N_2 atmosphere. The decomposition of pitch occurs between 350 – 500 ^{o}C.

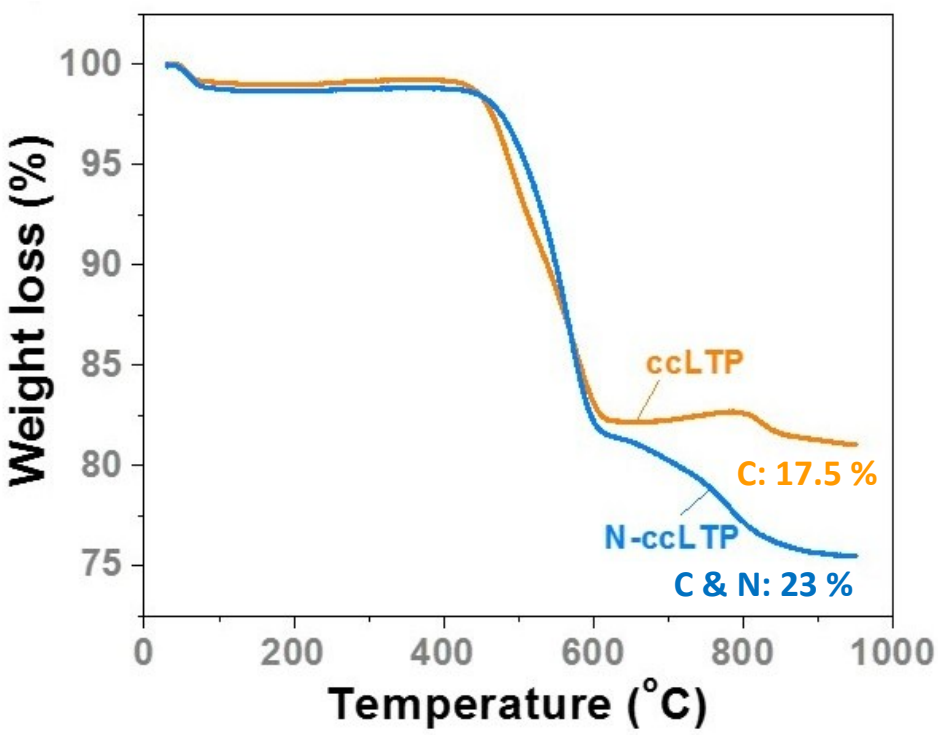

Figure S5. TGA spectra of N-ccLTP and ccLTP (prepared at 700 °C) in air. We note that the initial weight loss of ccLTP (c.a. 0.9%) and N-ccLTP (c.a. 1.2%) at temperatures between 50 to 100 °C are related to evaporation of water[2]. A slightly higher water content (Δ=0.3%) for N-ccLTP was observed compared to the ccLTP, which is attributed to the improvement of the surface hydrophilicity of the carbon layer by nitrogen doping[3, 4] leading to slightly more water absorbed onto the surface of N-ccLTP.

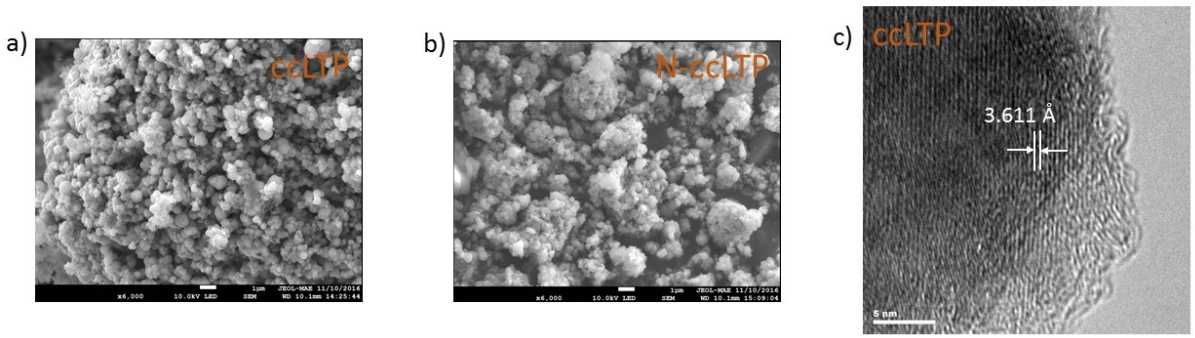

Figure S6. SEM images of (a) ccLTP and (b) N-ccLTP obtained at 700 °C. The scale bars are the same, i.e. 1 µm. (c) TEM image of ccLTP obtained at 700 °C. The scale bar is 5 nm.

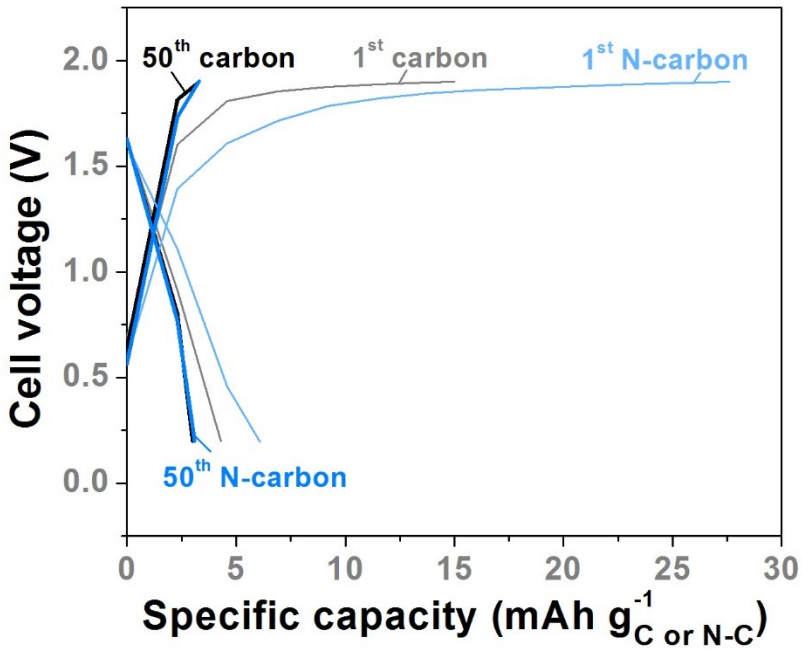

Figure S7. Electrochemical performance of the full cells using pure carbon and/or N-doped carbon as anodes and LMO as the cathode at the 138 mA per gram of anode materials (pure carbon or N-C). The carbon materials were prepared following the same procedure of preparing ccLTP and N-ccLTP at 700 °C without adding the LTP precursor.

Table S1. Summary of the state-of-the-art aqueous lithium-ion batteries.

Systems (+ve/-ve)	Ref	Electrolyte	C-rate performance**	Cycle performance
$LiFePO_4/LiTi_2(PO_4)_3$	5	1 M Li_2SO_4 (pH=13)	55 mAh g^{-1} @ 1 C *	90% retention after 1000 cycles @ 1 C
$LiMn_2O_4/Mo_6S_8$	6	21 m LiTFSI	40 mAh g^{-1} @ 0.15 C * 30 mAh g^{-1} @ 4.5 C *	72% retention after 1000 cycles @ 4.5 C
$LiNi_{0.5}Mn_{1.5}O_4/Mo_6S_8$	7	21 m LiTFSI	30 mAh g^{-1} @ 0.5 C * 17 mAh g^{-1} @ 5 C *	70% retention after 400 cycles @ 5 C
$LiCoO_2/Mo_6S_8$	8	21 m LiTFSI (0.1 wt% TMSB)	60 mAh g^{-1} @ 0.5 C * 38 mAh g^{-1} @ 2.5 C *	87% retention after 1000 cycles @ 2.5 C
$LiNi_{0.5}Mn_{1.5}O_4$/ $Li_4Ti_5O_{12}$	9	$Li(TFSI)_{0.7}$($BETI)_{0.3}$	25 mAh g^{-1} @ 6.8 C *	63% retention after 100 cycles @ 6.8 C
$LiMn_2O_4/TiO_2$	10	LiCl-Li_2SO_4	90 mAh g^{-1} @ 2 C 120 mAh g^{-1} @ 5 C (capacity based on the cathode)	NA
$LiFePO_4/LiFePO_4$	11	Sat. $LiNO_3$	116 mAh g^{-1} @ 2 C 50 mAh g^{-1} @ 8.5 C	80% retention after 500 cycles @ 1.1 C
$LiFePO_4$/graphite	12	LiSICON	138 mAh g^{-1} @ 0.5 C 80 mAh g^{-1} @ 5 C	95.8% retention after 24 cycles @ 0.3 C (50 mA g^{-1})
$LiMn_2O_4/LiTi_2(PO_4)_3$	13	2 M Li_2SO_4	112 mAh g^{-1} @ 0.1 C 40 mAh g^{-1} @ 20 C	90% retention after 300 cycles @ 0.22 C (30 mA g^{-1}) 84% retention after 1300 cycles @ 1.08 C (150 mA g^{-1})
$LiMn_2O_4/LiTi_2(PO_4)_3$	14	1 M Li_2SO_4	28 mAh g^{-1} @ 1.37 C * 8.3 mAh g^{-1} @ 68.5 C *	71% retention after 1000 cycles @ 1.4 C
$LiMn_2O_4/LiTi_2(PO_4)_3$	2	2 M Li_2SO_4	105 mAh g^{-1} @ 1 C 89 mAh g^{-1} @ 10 C	80.6% retention after 120 cycles @ 1 C 97% retention after 120 cycles @ 10 C
$LiMn_2O_4/LiTi_2(PO_4)_3$	15	2 M Li_2SO_4	123 mAh g^{-1} @ 1 C 103 mAh g^{-1} @ 10 C	91.2% retention after 100 cycles @ 0.22 C (30 mA g^{-1}) 90.4% retention after 400 cycles @ 1.08 C (150 mA g^{-1})
$LiMn_2O_4/LiTi_2(PO_4)_3$ **(This work)**		2 M Li_2SO_4	126 mAh g^{-1} @ 1 C 107 mAh g^{-1} @ 10 C 64 mAh g^{-1} @ 20 C	91.7% retention after 100 cycles @ 1 C (138 mA g^{-1}) 75% retention after 1000 cycles @ 5 C (690 mA g^{-1}) 67% retention after 1000 cycles @ 10 C (1380 mA g^{-1}) 58% retention after 2000 cycles @ 10 C (1380 mA g^{-1})

Notes: * Capacity calculation is based on total mass of active electrode materials.

**For those not specified, the capacity is based on the mass of the anode active material.

Table S2. Characteristics of the pitch (SBS-modified pitch). Data is supplied by Maoming Lu Sun Asphalt Co. Ltd, Guangdong, China. Identification number: 201605030009.

Test item	Quality index	Experimental result	Method
Softening point, °C	≥ 55	65	GB/T4507
Ductility, cm	≥ 30	36	GB/T4508
Penetration, 1/10 mm	60-80	68	GB/4509
Penetration index (PI)	≥ -0.4	-0.1	-
Viscosity, Pa · S	≤ 3	1.6	Viscosimeter
Flash point, °C	≥ 230	270	GB/T267
Solubility, %	≥ 99	99.5	GB/T11148
Separation, difference of softening point (163 °C, 48 h), °C	≤ 2.5	1.5	T0660-98
Elastic recovery (25 °C), %	≥ 65	78	T0661-98
After forming membrane: Mass change, %	≤± 1.0	0.1	GB/T5304
After forming membrane: Penetration ratio, %	≥ 60	70	GB/T4509
After forming membrane: Ductility (5 °C, 5 cm/min), cm	≥ 20	25	GB/T4508

Table S3. Comparison of different state-of-the-art flexible power sources.

System (+ve/-ve)	Electrolyte	Loading (mg cm^{-2})	Areal capacity (mAh cm^{-2})	Energy density (mWh cm^{-3})	Ref
Nonaqueous $LiCoO_2$/Li metal	LiPON	NA	0.05-0.1	2.2	16
Aqueous MnO_2/PEDOT:PSS	0.5 M Na_2SO_4	8.5	0.46	1.8	17
Nonaqueous $LiMn_2O_4/Li_4Ti_5O_{12}$	LiTFSI-PEO	NA	NA	17.7	18
Nonaqueous $LiMn_2O_4/Li_4Ti_5O_{12}$	$LiPF_6$ in EC:DEC	1-2	0.29	-	19
Aqueous MnO_2/Ni	Na_2SO_4-PVA	NA	0.53	0.78	20
Solid-state Reduced GO	Graphite oxide	NA	NA	0.43**	21
VO_x/VN	LiCl-PVA	0.71	NA	0.61	22
ZnO-doped MnO_2	LiCl-PVA	0.11	0.08	0.04	23
Aqueous Co_9S_8/Co_3O_4	KOH-PVA	2	0.65	1.21-1.44	24
Carbon nanotubes	H_3PO_4-PVA	NA	NA	0.701	25
Aqueous LIB $LiMn_2O_4/LiTi_2(PO_4)_3$	2 M $LiNO_3$	10-12	0.86-0.96	124	26
Aqueous LIB $LiMn_2O_4/LiTi_2(PO_4)_3$	2 M Li_2SO_4	10-12	1.2-1.4	26-31	**This work***

Notes: * The thickness of each component of the full cell was measured by caliper. The thickness of the cathode, anode and separator is determined to be 0.16 mm, 0.15 mm and 0.15 mm, respectively. The geometric active area of the cathode, anode and separator is 1 cm^2, 1 cm^2 and 2.25 cm^2, respectively. The energy is calculated by integrating the voltage vs. capacity plot.

** This value is obtained from the ref. 26.

Supplementary references

1. C. Xu, X. Cheng, L. Wang, J. Zhao, J. Wang and C. Song, The kinetics research on coal tar pitch and its extraction, 4th International Conference on Sensors, Measurement and Intelligent Materials (ICSMIM 2015), 2016, Shenzhen, China, 1004-1011.
2. Z. Liu, X. Qin, H. Xu and G. Chen, *J. Power Sources*, 2015, **293**, 562-569.
3. Y. Xue, J. Liu, H. Chen, R. Wang, D. Li, J. Qu and L. Dai, *Angew. Chem. Int. Ed.*, 2012, **51**, 12124-12127.
4. Y. Shao, X. Wang, M. Engelhard, C. Wang, S. Dai, J. Liu, Z. Yang and Y. Lin, *J Power Sources*, 2010, **195**, 4375-4379.
5. J.-Y. Luo, W.-J. Cui, P. He and Y.-Y. Xia, *Nat. Chem.*, 2010, **2**, 760-765.
6. L. Suo, O. Borodin, T. Gao, M. Olguin, J. Ho, X. Fan, C. Luo, C. Wang and K. Xu, *Science*, 2015, **350**, 938-943.
7. F. Wang, L. Suo, Y. Liang, C. Yang, F. Han, T. Gao, W. Sun and C. Wang, *Adv. Energy Mater.*, 2016, 1600922.
8. F. Wang, Y. Lin, L. Suo, X. Fan, T. Gao, C. Yang, F. Han, Y. Qi, K. Xu and C. Wang, *Energy Environ. Sci.*, 2016, **9**, 3666-3673.
9. Y. Yamada, K. Usui, K. Sodeyama, S. Ko, Y. Tateyama and A. Yamada, *Nat. Energy*, 2016, **1**, 16129.
10. S. Liu, S. Ye, C. Li, G. Pan and X. Gao, *J. Electrochem. Soc.*, 2011, **158**, A1490-A1497.
11. D. Gordon, M. Y. Wu, A. Ramanujapuram, J. Benson, J. T. Lee, A. Magasinski, N. Nitta, C. Huang and G. Yushin, *Adv. Energy Mater.*, 2016, **6**, 1501805.
12. Z. Chang, C. Li, Y. Wang, B. Chen, L. Fu, Y. Zhu, L. Zhang, Y. Wu and W. Huang, *Sci. Rep.*, 2016, **6**, 28421.
13. D. Sun, Y. Jiang, H. Wang, Y. Yao, G. Xu, K. He, S. Liu, Y. Tang, Y. Liu and X. Huang, *Sci. Rep.*, 2015, **5**, 10733.
14. J. Sun, Y. Sun, L. Gai, H. Jiang and Y. Tian, *Electrochim. Acta*, 2016, **200**, 66-74.
15. D. Sun, X. Xue, Y. Tang, Y. Jing, B. Huang, Y. Ren, Y. Yao, H. Wang and G. Cao, *ACS Appl. Mater. Interfaces*, 2015, **7**, 28337-28345.
16. M. Koo, K.-I. Park, S. H. Lee, M. Suh, D. Y. Jeon, J. W. Choi, K. Kang and K. J. Lee, *Nano Lett.*, 2012, **12**, 4810-4816.
17. Z. Su, C. Yang, C. Xu, H. Wu, Z. Zhang, T. Liu, C. Zhang, Q. Yang, B. Li and F. Kang, *J. Mater. Chem. A*, 2013, **1**, 12432-12440.
18. J. Ren, Y. Zhang, W. Bai, X. Chen, Z. Zhang, X. Fang, W. Weng, Y. Wang and H. Peng, *Angew. Chem.*, 2014, **126**, 7998-8003.
19. H. Xia, Q. Xia, B. Lin, J. Zhu, J. K. Seo and Y. S. Meng, *Nano Energy*, 2016, **22**, 475-482.
20. L. Zhang, P. Zhu, F. Zhou, W. Zeng, H. Su, G. Li, J. Gao, R. Sun and C.-p. Wong, *ACS Nano*, 2015, **10**, 1273-1282.
21. W. Gao, N. Singh, L. Song, Z. Liu, A. L. M. Reddy, L. Ci, R. Vajtai, Q. Zhang, B. Wei and P. M. Ajayan, *Nat. Nanotech.*, 2011, **6**, 496-500.
22. X. Lu, M. Yu, T. Zhai, G. Wang, S. Xie, T. Liu, C. Liang, Y. Tong and Y. Li, *Nano Lett.*, 2013, **13**, 2628-2633.
23. P. Yang, X. Xiao, Y. Li, Y. Ding, P. Qiang, X. Tan, W. Mai, Z. Lin, W. Wu and T. Li, *ACS Nano*, 2013, **7**, 2617-2626.
24. J. Xu, Q. Wang, X. Wang, Q. Xiang, B. Liang, D. Chen and G. Shen, *ACS Nano*, 2013, **7**, 5453-5462.

25. S. He, J. Cao, S. Xie, J. Deng, Q. Gao, L. Qiu, J. Zhang, L. Wang, Y. Hu and H. Peng, *J. Mater. Chem. A*, 2016, **4**, 10124-10129.
26. X. Dong, L. Chen, X. Su, Y. Wang and Y. Xia, *Angew. Chem. Int. Ed.*, 2016, **55**, 1-5.